

Available online at www.sciencedirect.com

SCIENCE @ DIRECT®

Nuclear Instruments and Methods in Physics Research B 234 (2005) 148–158

NIM B
Beam Interactions
with Materials & Atomswww.elsevier.com/locate/nimb

Dynamical diffraction theory for the parametric X-rays and coherent bremsstrahlung

I. Feranchuk^{a,*}, O. Lugovskaya^a, A. Ulyanenkov^b^a *Belarusian State University, Fr. Skaryny Av., 4, 220050 Minsk, Belarus*^b *Bruker AXS, Östliche Rheinbrückenstr. 49, 76187 Karlsruhe, Germany*

Received 7 September 2004; received in revised form 1 February 2005

Available online 23 March 2005

Abstract

The various mechanisms of X-ray radiation from relativistically charged particles in a crystal are analyzed from a common point of view, based on quantum electrodynamics in a medium. Parametric X-rays (PXR), diffraction radiation (DR) and coherent bremsstrahlung (CB) lead to different contributions to the amplitude of the radiation process but because of their interference they cannot be considered separately in the radiation intensity. The role of the dynamical diffraction effects and the coherent bremsstrahlung is considered to be dependent on the crystal parameters and particle energy. The conception of the high resolution parametric X-rays (HRPXR) is introduced and the universal radiation distribution, which can simplify the analysis of the results for this case is also considered. The possible applications of HRPXR are discussed.

© 2005 Elsevier B.V. All rights reserved.

PACS: 41.50.+h; 41.60.–m

Keywords: Parametric X-ray; Coherent bremsstrahlung; Diffraction

1. Introduction

In the last decade a series of problems connected with X-ray production from relativistically

charged particles (more specifically, electrons) in a crystal were discussed by many authors. These problems can be divided into the following groups: (1) the role of the dynamical diffraction effects in these processes; (2) the contributions of the various radiation mechanisms to the total intensity and (3) which applications of the X-ray radiation from the relativistic electrons in a crystal could be most essential?

* Corresponding author. Tel.: +375 172 277617; fax: +375 172 202353.

E-mail address: fer@open.by (I. Feranchuk).

Meanwhile, it seems important to recall that analogous questions have already been considered quite long ago in a series of publications of Baryshevsky, Feranchuk and co-authors. In particular, the general theory of X-ray radiation from relativistic electrons in a crystal taking into account the various mechanisms of the photon production and their dynamical diffraction have been formulated in [1]. The influence of dynamical effects on the formation of the fine structure of the PXR peaks was considered for the forward direction [2,3], for a highly asymmetrical case [4], for degenerate diffraction in the case of backward Bragg geometry [5]. The possible advantages and shortcomings of the PXR as the source of X-rays in comparison with other radiation mechanisms in the same wavelength range were discussed in [6]. It has also been shown that PXR could be mainly important for spectral sensitive applications, that is, for the cases where only high spectral intensity in the narrow wavelength range is important. Some non-trivial physical problems of such type are considered in [7–9] and a series of them have been described in detail in [10,11].

It is essential to note that the above mentioned results concerning PXR features were theoretical predictions made before the experimental confirmation. Some of them initiated the first observations of the PXR peaks [12] and their angular distribution [13]. A simplified model for the description of the PXR characteristics was suggested in [14]. At present there are a lot of experimental works in this field (see [15–17] for recent ones and references therein) and most of their results are in qualitative agreement with the predictions of [14] with a rather small deviation in their quantitative details. Essential contribution to the detailed analysis of this phenomenon was made in many theoretical works (for example, [18–24] and references therein).

The series of qualitatively different experimental works which has appeared recently (for example, [25]) can open up an essentially new side in the PXR investigations and applications. The two-crystal schemes of the detector was used for very high energy resolution of the emitted photon spectrum. In some sense this is analogous to the essential extension of the applications of the

conventional diffractometry due to high resolution X-ray diffraction (HRXRD) which is now very important part of modern semiconductor and nanostructure technology [26]. Therefore it becomes necessary to discuss in more detail the general approach for description of dynamical effects in the formation of X-ray spectra from charged particles in crystals. The fine structure of such spectra can be considered as a high resolution parametric X-radiation (HRPXR) and it should be represented in some universal form as was done for the kinematical PXR [14]. It will help us to analyze the experimental data and consider possible applications of HRPXR.

The present report is organized as follows. In Section 2 we will shortly discuss the special diagrammatic technique for calculating amplitudes of any radiation process in a crystal when interaction of the photons and charged particles with the medium is considered without the perturbation theory. The electron wave function and the radiation wave field in a crystal are calculated in Section 3. The relation between the amplitudes of various radiation processes is considered in Section 4. The special scale, dimensionless parameters and universal curves for the analysis of HRPXR are introduced in Section 5 and possible applications of HRPXR are discussed.

2. Quantum electrodynamics in crystals

We will calculate the cross-sections of various electromagnetic processes in a crystal on the basis of the special representation of quantum electrodynamics (QED) [1]. The system of units with the Plank constant \hbar and the light velocity c

$$\hbar = c = 1,$$

and the fine structure constant $e^2 \simeq 1/137$. Let us also select the ranges of the electron energy E and the photon frequency ω which are most essential for the problem considered

$$E \geq 50 \text{ MeV}, \quad \omega \sim 2\text{--}20 \text{ keV}.$$

According to [6], the electron energy in this range is optimal for X-ray production in a crystal.

It is clear that recoil effects are not important in radiation processes with such ratios of photon and electron energies and classical formulas are also applicable. But it will be shown below that the QED approach is more preferable because: (a) actually the quantum calculations are not more complicated than classical ones but remain correct for any energies, (b) it permits one to make classification of various radiation processes clearer and (c) it does not necessitate solving the inhomogeneous Maxwell equations in order to calculate the radiation intensity as taking place in classical electrodynamics.

The quantum description of the electromagnetic processes in a crystal is based on the following representation of the Hamiltonian of the system:

$$\hat{H} = \hat{H}_{e,c} + \hat{H}_{\gamma,c} + \hat{H}_{e,\gamma}, \quad (1)$$

which differs from the vacuum QED [27], because the Hamiltonians for the electron and photon subsystems include both the operators \hat{H}_e , \hat{H}_γ of the free fields and the coherent potentials of their interaction with a crystal. Therefore, the second quantization of these fields is based not on the vacuum plane waves but on the one-particle eigenfunctions of the operators $\hat{H}_{e,c}$, $\hat{H}_{\gamma,c}$.

Particularly, the wave functions $\Psi_E^\pm(\vec{r})$ for the electron states with the energy E and other quantum numbers ν are defined as the solutions of the Dirac equation

$$[(\vec{\alpha}\vec{p}) + \beta m + U(\vec{r}) - E] \Psi_{\nu E}^\pm(\vec{r}) = 0. \quad (2)$$

Here α_i , β are Dirac's matrices; $\vec{p} = -i\vec{\nabla}$ is the momentum operator; index (\pm) corresponds to the wave functions including asymptotically outgoing (ingoing) spherical waves which are used for the electrons in the initial (final) states [1,27]. Potential $U(\vec{r})$ describes the coherent interaction of the electron with the periodical field of a crystal and can be expressed through the amplitudes of its elastic scattering at the atom of the crystal unit cell [28]:

$$U(\vec{r}) = \sum_{\vec{h}} U_{\vec{h}} e^{i\vec{h}\vec{r}} H(z)H(L-z),$$

$$U_{\vec{h}} = -\frac{4\pi e^2}{h^2 \Omega} \sum_j [Z_j - F_j(\vec{h})] e^{i\vec{h}\vec{R}_j} e^{-W_j(\vec{h})}, \quad (3)$$

where \vec{h} is the reciprocal lattice vector; \vec{R}_j is the coordinate of the atom with index j in the cell; Z_j , $F_j(\vec{h})$ are its nucleus charge and atomic scattering factor correspondingly; $e^{-W_j(\vec{h})}$ is the Debye–Waller factor and Ω is the volume of the unit cell.

It is important to note that the known forms of QED in a medium (for example, Farry representation [27]) were usually considered without taking into account the finite size of the medium. In our approach the full set of the states for QED in the crystal should be constructed for the finite thickness L of the crystal which we took into account by means of the Heaviside functions $H(z)$ and $H(L-z)$ in formula (3) and the corresponding boundary conditions for the wave functions.

In turn, the stationary states of the electromagnetic field with frequency ω and quantum numbers μ in the crystal are defined by the vector potentials $\vec{A}_{\mu\omega}^\pm(\vec{r})$ which are the solutions of the Maxwell equations with the periodical permittivity of the crystal [1]:

$$\epsilon_{ij}(\vec{r}, \omega) = \delta_{ij} + \chi_{ij}(\vec{r}, \omega) H(z)H(L-z). \quad (4)$$

The susceptibility $\chi_{ij}(\vec{r}, \omega)$ is well known for X-ray wavelengths [26]:

$$\chi_{ij}(\vec{r}, \omega) = \delta_{ij} \sum_{\vec{h}} \chi_{\vec{h}} e^{i\vec{h}\vec{r}},$$

$$\chi_{\vec{h}} = -\frac{4\pi e^2}{m\omega^2 \Omega} \sum_j [F_j(\vec{h}) + f'(\omega) + if''(\omega)] \times e^{i\vec{h}\vec{R}_j} e^{-W_j(\vec{h})}, \quad (5)$$

with the f' and f'' as the anomalous dispersion corrections. The entire data base for the calculation of $\chi_{\vec{h}}$ was described recently in the paper [29].

The Hamiltonian $\hat{H}_{e,\gamma}$ for the interaction between the electron and electromagnetic fields in a crystal has the same form as in the vacuum QED [27]

$$\hat{H}_{e,\gamma} = e \int d\vec{r} \hat{\Psi}^*(\vec{r}) (\vec{\alpha}\vec{A}(\vec{r})) \hat{\Psi}(\vec{r}), \quad (6)$$

but with the field operators which are represented as a series in the annihilation and creation operators corresponding to the states $\Psi_{\nu E}^\pm(\vec{r})$, $\vec{A}_{\mu\omega}^\pm(\vec{r})$ instead of the plane waves [11]:

$$\widehat{\Psi}(\vec{r}) = \sum_{\nu} [b_{\nu} \Psi_{\nu E}^{-}(\vec{r}) + b_{\nu}^{+} \Psi_{\nu E}^{+}],$$

$$\vec{A}(\vec{r}) = \sum_{\mu} [a_{\mu} \vec{A}_{\mu\omega}^{-}(\vec{r}) + a_{\mu}^{+} \vec{A}_{\mu\omega}^{+}]. \quad (7)$$

Analogously to the vacuum QED, the amplitude of any electromagnetic process in the crystal, homogenous media or in some external field can be calculated by means of the perturbation theory on the operator $\widehat{H}_{e,\gamma}$. It leads to the same form of the diagrammatic representation for these amplitudes but with some change of the physical sense of the lines on the diagrams: instead of thin lines corresponding to the plane waves in the vacuum QED, one should use thick lines which define the wave functions of the particle or the photon taking into account in some non-perturbative way their interaction with the media. Each diagram uses the same vertex as for the vacuum QED. If one does not consider the many-photon processes, the Feynman diagrams of the first order are most essential and are actually enough to calculate the cross-section of any known electromagnetic process. Some examples of the diagrams are shown in Fig. 1. In particular, diagram (a) corresponds to the vacuum QED and this process, evidently, is forbidden because of the conservation laws of momentum and energy [27]. But for all other diagrams the conservation law for momentum does not fulfilled because of the external potential and they describe the amplitudes of the real physical processes: Fig. 1(b) defines the Cherenkov radiation in the homogeneous media with the constant refraction index n ; Fig. 1(c) corresponds to the

synchrotron radiation from the electron in the magnetic field \vec{H} ; Fig. 1(d) can be used for calculation of the PXR amplitude; Fig. 1(e) describes the amplitude as the coherent bremsstrahlung as the radiation from the channeled particles and Fig. 1(f) corresponds to the most general case of the radiation in a crystal.

The rules for identification of the diagram with the analytical expression for the amplitude of the concrete process are the same as in vacuum QED except momentum conservation. As for example, the analytical expression for the amplitude corresponding to Fig. 1(f) is as follows [1]:

$$M_{fi} = \delta(E - E_1 - \omega) T_{fi},$$

$$T_{fi} = \int d\vec{r} (\Psi_{\nu_1 E_1}^{-})^* (\vec{\alpha} \vec{A}_{\mu\omega}^{-})^* (\Psi_{\nu E}^{+}). \quad (8)$$

The considered sketch for the QED in media is sufficient to make clear the technique of the calculations for the sections.

3. Analytical expressions for the wave function and vector potential

Certainly, Eq. (8) is not the full solution of the problem considered because one should find the appropriate expression for the electron and photon eigenstates. In the general case one should use some approximation for the solution of the corresponding equations but it is important that these equations are homogeneous in the considered quantum approach [10,11] as distinct from the classical calculation [30].

Let us find firstly the electron wave function as the solution of Eq. (2). The following condition is fulfilled for real crystals:

$$\|U(\vec{r})\| \sim 1 \text{ eV}, \quad \|U(\vec{r})\| \ll E. \quad (9)$$

Eq. (2) can be “squared” in order to exclude the most of the spinor operators [27] and with an accuracy of $(U/E)^2$ it leads to

$$\left[-\Delta + m^2 - E^2 + 2EU(\vec{r}) - i(\vec{\alpha}\vec{V})U(\vec{r}) \right] \Psi_E(\vec{r}) = 0. \quad (10)$$

In the first stage we should find the stationary states in the infinite crystal and can use for this

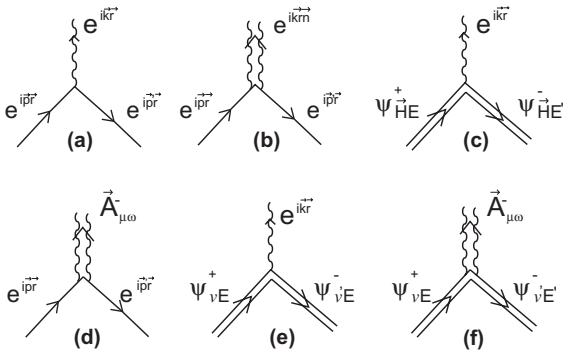


Fig. 1. Feynman diagrams for quantum electrodynamics in media.

calculation the perturbation theory (PT) because of the condition (9)

$$\begin{aligned}\Psi_E(\vec{r}) &\equiv \Psi_0 + \sum_{\vec{h} \neq 0} \Psi_{\vec{h}} \approx e^{i\vec{p}\vec{r}} \left[1 + \sum_{\vec{h} \neq 0} \widehat{B}_{\vec{h}} e^{i\vec{h}\vec{r}} \right] \chi_E, \\ \widehat{B}_{\vec{h}} &= -\frac{2E + (\vec{\alpha}\vec{h})}{2(\vec{p}\vec{h}) + h^2} U_{\vec{h}}, \\ p_z &= \sqrt{E^2 - m^2 - p_{\perp}^2},\end{aligned}\quad (11)$$

with χ_E as the bispinor corresponding to the free electron [27].

It is well known for this problem that PT is unapplicable for the special geometry when the particle momentum is perpendicular to some sets of the reciprocal lattice vector $(\vec{p}\vec{h}) \approx 0$. This case corresponds to the electron channeling and the non-perturbative method should be used for the solution of Eq. (2) taking into account the zone spectrum for the transversal movement [10,31]. But the special case of the channeling is not essential for our consideration and we will further suppose that $(\vec{p}\vec{h}) \neq 0$ and approximation (11) can be simplified because of the condition

$$2(\vec{p}\vec{h}) \gg h^2. \quad (12)$$

The next step is to use the continuity conditions for the wave function on the crystal boundaries $z = 0$, $z = L$. Calculation leads to the following results:

$$\begin{aligned}\Psi_E^{(\pm)} &\approx e^{i\vec{p}\vec{r}} \left[1 + \varphi_E^{(\pm)}(\vec{r}) \right] \chi_E, \\ \varphi_E^{(+)} &= \sum_{\vec{h} \neq 0} \widehat{B}_{\vec{h}} e^{i\vec{h}\vec{r}} \{ C_h(z) H(z) H(L-z) \\ &\quad + C_h(L) H(z-L) \}, \\ C_h(z) &= 1 - \exp[i(\tilde{p}_h - p_z - h_z)z], \\ \tilde{p}_h &= \sqrt{E^2 - m^2 - (\vec{p}_{\perp} - \vec{h}_{\perp})^2}, \\ \varphi_E^{(-)} &= \sum_{\vec{h} \neq 0} \widehat{B}_{-\vec{h}} e^{-i\vec{h}\vec{r}} \{ C_{-h}(z-L) H(z) H(L-z) \\ &\quad + C_{-h}(-L) H(-z) \}.\end{aligned}\quad (13)$$

It should be noted that the non-perturbed plane wave includes the functions $\Psi_E^{(\pm)}$ from the left and right sides of the crystal correspondingly.

An analogous problem for the vector potential $\vec{A}_{\mu\omega}^{\pm}(\vec{r})$ should be solved taking into account the diffraction of the emitted photon and the standard boundary conditions for the field on the interfaces of the crystal. In the case of the function $\vec{A}_{\mu\omega}^+(\vec{r})$ it is equivalent to the conventional X-ray diffraction problem [26]. The function $\vec{A}_{\mu\omega}^-(\vec{r})$ with another asymptotic can be calculated by means of relation [1]

$$\vec{A}_{\vec{k}\omega}^-(\vec{r}) = \left[\vec{A}_{-\vec{k}\omega}^+(\vec{r}) \right]^* \quad (14)$$

which is the analog of the well known ‘‘reciprocity theorem’’. So, we can refer to the results of the dynamical diffraction theory [26] without discussion of the details. As for example and in order to introduce the necessary notations, here we write the expression only for $\vec{A}_{\mu\omega}^+(\vec{r})$ calculated in the two-beam approximation and for the Bragg boundary conditions [26], corresponding to the experiment [25]. The vector potentials for other cases were described in [1,10] and for many-beam diffraction in [22]. Fig. 2 shows the distribution of the primary $\vec{A}_{\vec{k}}$ and diffraction $\vec{A}_{\vec{k}}$ wave fields and their normalized analytical representations are

$$\begin{aligned}\vec{A}_{\vec{k}\omega}^{(+s)}(\vec{r}) &\equiv \vec{A}_{\vec{k}} + \vec{A}_{\vec{h}} \\ &= \sqrt{\frac{2\pi}{\omega}} e^{i\vec{k}\vec{r}} \left\{ (\vec{e}_s + \vec{e}_{sh} e^{i\vec{h}\vec{r}} D_{sh}(L)) H(-z) \right. \\ &\quad + (\vec{e}_s D_{s0}(L-z) \\ &\quad + \vec{e}_{sh} e^{i\vec{h}\vec{r}} D_{sh}(L-z)) H(z) H(L-z) \\ &\quad \left. + \vec{e}_s D_{s0}(L) H(z-L) z \right\}, \\ D_{s0}(z) &= -\sum_{\mu=1}^2 \gamma_{\mu s}^0 \exp \left[i\omega \epsilon_{\mu s} \frac{L}{\gamma_0} \right], \\ D_{sh}(z) &= \beta \sum_{\mu=1}^2 \gamma_{\mu s}^h \exp \left[i\omega \epsilon_{\mu s} \frac{L}{\gamma_0} \right].\end{aligned}\quad (15)$$

Here we use the standard notations from the dynamical diffraction theory [26]: \vec{e}_s, \vec{e}_{sh} ; $s = 1, 2$ are the polarization vectors for the primary and diffraction waves; $\gamma_0 = (\vec{k}\vec{N})/k$ with \vec{N} as the unit vector of the normal to the crystal surface; $\beta = \gamma_0/\gamma_h$; $\gamma_h = (\vec{k}_h\vec{N})/k_h$; $\vec{k}_h = \vec{k} + \vec{h}$ (Fig. 2). The solutions of the dispersion equation which defines the refraction of the waves in a crystal are

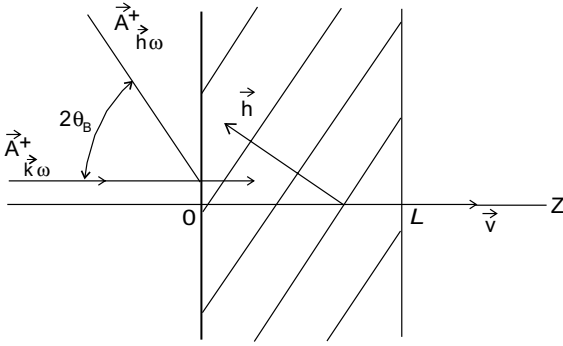


Fig. 2. Directions of the wave propagations for the diffraction in the Bragg geometry.

expressed by means of the components of the susceptibility (5) and has the following form [25]:

$$\epsilon_{\mu s} = \frac{1}{4} \left\{ -\alpha_B + \chi_0(\beta + 1) \pm \sqrt{[-\alpha_B + \chi_0(\beta - 1)]^2 + 4\beta C_s^2 \chi_h \chi_{-h}} \right\},$$

$$C_s = \cos 2\theta_B; \quad \sin \theta_B = \frac{h}{2k}; \quad \alpha_B = \frac{2\vec{k}\vec{h} + h^2}{k^2}. \quad (16)$$

The dimensionless value α_B is very important for the diffraction theory, in our case it characterizes the deviation of the wave vector of the emitted photon from the exact Bragg condition corresponding to $\alpha_B = 0$. Additional parameters in Eq. (15) were appeared because of the boundary condition and in the Bragg case considered they are defined as follows:

$$\gamma_{1(2)s}^0 = \frac{2\epsilon_{2(1)s} - \chi_0}{2(\epsilon_{2(1)s} - \chi_0) - 2(\epsilon_{1(2)s} - \chi_0) \exp[i\omega(\epsilon_{2(1)s} - \epsilon_{1(2)s})L/\gamma_0]},$$

$$\gamma_{1(2)s}^h = \frac{-\beta C_s \chi_h}{2(\epsilon_{2(1)s} - \chi_0) - 2(\epsilon_{1(2)s} - \chi_0) \exp[i\omega(\epsilon_{2(1)s} - \epsilon_{1(2)s})L/\gamma_0]}. \quad (17)$$

Formulas (11)–(17) for eigenfunctions look a little bit inconvenient because of the different representations inside and outside of the crystal. But we stress that all these parts of the functions should be taken into account while calculating the matrix element (8) in order to describe all

essential radiation processes. As for example, the method used recently in [20] for the dynamical effects in PXR does not permit one to describe the so-called diffraction transition radiation [25] which can be considered actually as the part of the PXR amplitude (see Section 4).

4. Intensity of the PXR + CBS radiation

The number of photons emitted within the spectral interval $d\omega$ and with the angular spread $d\Omega$ from one electron in the crystal is expressed through the matrix element (8) by means of the standard rules of QED [27]

$$\frac{\partial^2 N}{\partial \omega \partial \Omega} = \omega^2 \int |T_{fi}|^2 \delta(E - E_1 - \omega) \frac{d\vec{p}_1}{(2\pi)^6}, \quad (18)$$

where the integration over the E_1, \vec{p}_1 as the energy and momentum of the electron in the final state is supposed.

As was qualitatively illustrated in our papers [1,14] the angular distribution from the relativistic electron is separated actually to the narrow peak with an angular width $\Delta\theta \sim m/E$ along the electron velocity and to the set of non-overlapping peaks (reflexes) with the analogous angular widths along the directions corresponding to the various reciprocal lattice vectors \vec{h} and each of these reflexes can be analyzed independently. Fig. 3 shows those three diagrams which give the contribution to one of such side reflexes. Fig. 3(a) corresponds to the diffraction of the emitted photon that is to the amplitude of PXR. Fig. 3(b) and (c) describes the amplitudes of CBS conditioned by the diffraction of the electron in the initial or the final states correspondingly. This representation makes the physical difference between the processes clearer

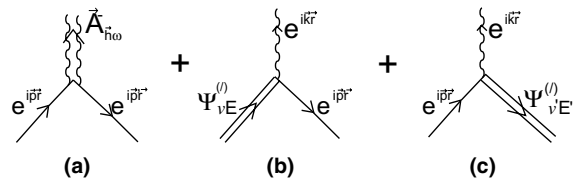


Fig. 3. Diagrams for the (CBS + PXR) radiation.

in both cases there is quite a big momentum transfer when producing the photon with the wave vector $(\vec{k} + \vec{h})$, but in the PXR case, the recoil is received by the crystal during the photon diffraction and in the CBS process it is compensated by the change in the electron momentum due to the diffraction by the crystallographic planes with the reciprocal lattice vector $(-\vec{h})$. It is interesting to note that the electron diffraction itself cannot be resolved for the considered relativistic energy E (all of them are in the very small cone along the electron velocity) but one can see its secondary effect as the CBS peaks. This is possible because the small scattering angle for electrons leads to the large angle for the emitted photons due to the condition $E \gg m$.

The wave functions corresponding to the lines of the diagrams from Fig. 3 for the Bragg geometry considered are defined by Eqs. (11) and (15). A not very complicated calculation of the matrix elements with the average over the initial electron spin states and the summation over its final ones [27] leads to the following expression (the intensities of the photons with different polarization $s = 1, 2$ can be considered separately):

$$\begin{aligned} \frac{\partial^2 N_{hs}}{\partial \omega \partial \Omega} &= \frac{e^2 \omega}{4\pi^2} (\vec{\epsilon}_{hs} \vec{v}_h)^2 |M_{\text{PXR}} + M_{\text{CBS}}|^2, \\ M_{\text{PXR}} &= \sum_{\mu=1}^2 \gamma_{\mu s}^h \left(\frac{1}{q_{0h}} - \frac{1}{q_{\mu hs}} \right) [\exp(iq_{\mu hs} L / \gamma_1) - 1], \\ M_{\text{CBS}} &= - \frac{U_{-\vec{h}}}{(\vec{v}\vec{h})} \frac{[\exp(iq_{0h} L / \gamma_1) - 1]}{q_{0h}}, \\ \vec{v}_h &= \left(\vec{v} + \frac{\vec{h}}{\omega} \right), \quad q_{0h} = [\omega - (\vec{v}\vec{k}_{-h})] / v, \\ \vec{k}_{-h} &= \vec{k} - \vec{h}, \quad q_{\mu hs} = [\omega - (\vec{v}\vec{k}_{-h\mu s})] / v, \\ \vec{k}_{-h\mu s} &= \vec{k} - \vec{h} + \omega \epsilon_{\mu s} \vec{N} / \gamma_0. \end{aligned} \quad (19)$$

Only the leading terms in a power series of the parameters U/E and h/E are taken into account in M_{CBS} . The values $L_{0h} = 1/q_{0h}$ and $L_{\mu hs} = 1/q_{\mu hs}$ are known as the radiation coherent lengths for the vacuum and crystal correspondingly. The PXR matrix element actually includes the coherent superposition of both coherent lengths. It was suggested in some papers (for example, [25]) to

consider the contribution, which is proportional to L_{0h} and conditioned by the crystal boundary, as a special radiation mechanism (diffraction transition radiation). But it seems to us that such a separation is not very rigorous in the radiation intensity and we further consider M_{PXR} as the single amplitude of the process conditioned by the diffraction of the emitted photons in a crystal.

One can see from formula (19) that the total radiation intensity is defined by the interference of the PXR and CBS amplitudes. This phenomenon was firstly discussed theoretically in [32]. A more detailed calculation and analysis of the spectral-angular distribution of both radiation mechanisms were fulfilled in [33]. The theory and experimental investigation of PXR and CBS interference were also considered in [34].

All the above-mentioned results were referred to the case of relativistic electrons. However, as was shown in our paper [35], the PXR and CBS interference is the most essential for the non-relativistic electrons when the angular distribution for both radiation mechanisms are undistinguishable. Formula (19) coincides with the results from [32,34] in the corresponding limit cases $E \gg m$ but it can actually be used in the entire range of the electron energy, even in the case $\omega \sim E$ considered in [35]. Besides, it takes into account the crystal boundaries which lead to the term q_{0h}^{-1} omitted in the above-mentioned papers. This contribution corresponds to the diffraction transition radiation (DR) and may be essential in some range of angles (see Section 5). If the radiation of the hard photon ($\omega \sim E \gg m$) should be calculated, the refraction and diffraction of the electromagnetic field are unessential. In this case only the amplitude M_{CBS} is important in (19) and it leads to well known results [37].

In this paper the case of ultrarelativistic electrons is of interest and it is possible to find the simple analytical estimation for the relative contributions of both the intensities. The amplitude M_{PXR} is the most essential in the spectral ($\Delta\omega/\omega$) and angular ($\Delta\theta$) intervals where the wave vector of the emitted photon satisfies the Bragg condition. In this case the parameters in formulas (16) and (17) are estimated as

$$\alpha_B \simeq \Delta\omega/\omega \simeq |\chi_{\vec{h}}|, \quad |\gamma_{\mu s}^h| \simeq 1.$$

In this narrow range the PXR contribution to the angular-spectral distribution has an order of the magnitude

$$\left(\frac{\partial^2 N}{\partial \omega \partial \Omega}\right)_{\text{PXR}} \approx \frac{e^2}{4\pi} (\vec{e}_{hs} \vec{v}_h)^2 \omega L_{0h}^2. \quad (20)$$

At the same time its contribution to the integral intensity of the reflex is defined as follows [14]:

$$N_{\text{PXR}} \approx \frac{e^2}{4\pi} \frac{|\chi_h|^2}{\sin^2 \theta_B} \omega_B L_a [1 - \exp(-L/L_a)], \quad (21)$$

where L_a is the crystal absorption length for the X-rays with a frequency $\omega_B = h/\sin \theta_B$, corresponding to the Bragg frequency in the PXR reflex [14].

The analogous estimations for the CBS contribution leads to

$$\left(\frac{\partial^2 N}{\partial \omega \partial \Omega}\right)_{\text{CBS}} \approx \frac{e^2}{4\pi} (\vec{e}_{hs} \vec{v}_h)^2 \omega L_{0h}^2 \left|\frac{U_{\vec{h}}}{h}\right|^2, \\ \left|\frac{U_{\vec{h}}}{h}\right| \leq 10^{-2}, \\ N_{\text{CBS}} \approx \frac{e^2}{4\pi} \frac{m^2}{E^2} \left|\frac{U_{\vec{h}}}{h}\right|^2 \omega L_a [1 - \exp(-L/L_a)]. \quad (22)$$

This means that the maximal spectral intensity of PXR is of several orders larger than the analogous one for CBS, but CBS can give a noticeable contribution to the integral intensity of the reflex. If one takes into account Eqs. (3) and (5) for the components of the potential and susceptibility the ratio of the CBS and PXR intensities in the same reflex can be calculated

$$\xi = \frac{N_{\text{CBS}}}{N_{\text{PXR}}} \approx \left[\frac{Z - F(\vec{h})}{F(\vec{h})}\right]^2 \left(\frac{m^2}{Eh}\right)^2 \frac{1}{16\sin^4 \theta_B}. \quad (23)$$

In other words, the CBS contribution should be taken into account in the following electron energy range:

$$E \leq \left|\frac{Z - F(\vec{h})}{F(\vec{h})}\right| \left(\frac{m^2}{4h\sin^2 \theta_B}\right). \quad (24)$$

This estimation is in qualitative agreement with the results of [34]. It also shows that in the considered energy range ($E \geq 50$ MeV) in this work this radiation mechanism is not very important except the case of the high-order harmonics when the

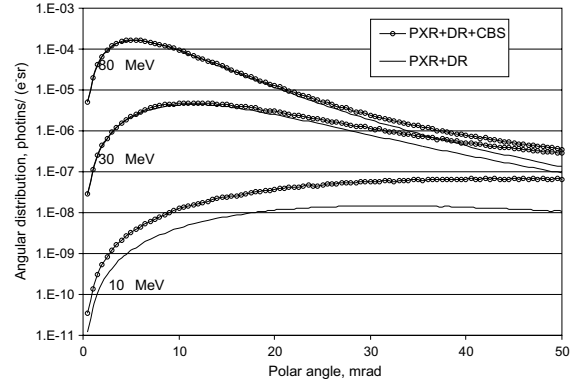


Fig. 4. Contribution of CBS to the radiation intensity in dependence on the electron energy.

atomic scattering factor $F(\vec{h})$ can be exponentially small.

The accurate analysis of the contributions of PXR, CBS and their interference to the integral intensity of the reflex is connected with the numerical integration on the basis of formula (19). Fig. 4 shows the contributions of PXR alone and totally (PXR + DR + CBS) to the integral intensity of the reflex for the experimental conditions corresponding to those in [36]. The intensity of the reflex in the Bragg backward geometry was calculated as the function of the angle ψ between the electron velocity \vec{v} and the crystal surface normal \vec{N} in the vicinity of $\psi = 0$ [36]. One can see that the effect of CBS is almost negligible for the electron energy $E = 85$ MeV but becomes important for $E = 30$ MeV.

5. Analysis of the dynamical diffraction effects in the case of HRPXR

In this section we will analyze the general formula (19) in the narrow angular-spectral range where the dynamical effects could appear. As was mentioned above the CBS matrix element can be omitted in this case. Let us also introduce for the PXR reflex (\vec{h}) the special coordinate system where the frequency ω and the angles θ , φ of the emitted photons are counted relatively to the vector \vec{k}_B when the Bragg condition ($\alpha_B = 0$) is satisfied exactly. In these variables the photon wave vector

\vec{k} with an accuracy of $|\chi_{\vec{h}}| \leq 10^{-5}$ can be written as [11]:

$$\begin{aligned}\vec{k} &= \vec{k}_B + \delta\vec{k}, \\ \delta\vec{k} &= \delta\omega\vec{n}_B + \omega_B\theta(\vec{n}_x \cos\varphi + \vec{n}_y \sin\varphi), \\ \delta\omega &= \omega - \omega_B, \quad \vec{k}_B = \omega_B\vec{v} + \vec{h}, \\ \omega_B &= \frac{h}{2v|\sin\theta_B|}, \quad \vec{n}_B = \frac{\vec{k}_B}{k_B}, \quad \theta_B = \frac{1}{2}\widehat{v\vec{n}_B},\end{aligned}\quad (25)$$

and the unit vectors \vec{n}_x, \vec{n}_y are in the plane perpendicular to \vec{n}_B .

One can express the most essential values in Eq. (19) by means of these variables with the same accuracy:

$$\begin{aligned}\alpha_B &= 4\frac{\delta\omega}{\omega_B}\frac{\sin^2\theta_B}{\cos 2\theta_B} - 2\theta \sin\varphi \tan 2\theta_B, \\ \gamma_0 &= (\vec{v}\vec{N}), \quad \gamma_1 = (\vec{n}_B\vec{N}), \\ q_{0h} &= \frac{1}{2}\omega_B[\theta^2 + \theta_{ph}^2], \\ q_{\mu hs} &= \frac{1}{2}\omega_B[\theta^2 + \theta_{ph}^2 - 2\epsilon_{\mu s}], \\ (\vec{e}_{hs}\vec{v}_h)^2 &= \theta^2 v_s, \\ v_{1(2)} &= \sin^2\varphi(\cos^2\varphi), \\ \theta_{ph}^2 &= \frac{m^2}{E^2} + \theta_{sc}^2 + \theta_M^2.\end{aligned}\quad (26)$$

Analogously to the model [14] we have introduced here the value θ_{ph}^2 in order to take into account qualitatively the influence of the electron multiple scattering (θ_{sc}^2) and the crystal mosaicity (θ_M^2) on the formation of the PXR reflex.

Eq. (19) can be used for any crystal thickness L . Particularly, if $L < L_{\text{ext}} \simeq (\omega_B\chi_0)^{-1}$ (L_{ext} is the extinction length), this formula takes the same form as in the kinematical diffraction theory which was analyzed earlier in our paper [14]. Therefore in this paper we consider the opposite case $L > L_{\text{ext}}$ when the dynamical effects are supposed to be essential for HRPXR analogously to the conventional high resolution X-ray diffraction (HRXRD) [26]. Moreover, in order to make more clear the specific features of the HRPXR peaks let us consider the case of the thick crystal with $L > L_{\text{abs}} \simeq (2\omega_B\Im\chi_0)^{-1}$ (L_{abs} is the absorption length) when the oscillation structure of the diffraction peaks does not appear [26].

With this supposition the only root with $\Im\epsilon_{\mu s} > 0$ of Eq. (16) is essential and Eq. (19) is essentially simplified

$$\begin{aligned}\frac{\partial^2 N_{hs}}{\partial\omega\partial\Omega} &= \frac{e^2}{\omega_B\pi^2}\theta^2 \left| \frac{\beta C_s v_s \chi_{\vec{h}}}{2\epsilon_{1(2)} - \chi_0} \right|^2 \left| \frac{1}{\theta^2 + \theta_{ph}^2} - \frac{1}{\theta^2 + \theta_{ph}^2 - 2\epsilon_{1(2)s}} \right|^2,\end{aligned}\quad (27)$$

where the index 1(2) for various ω, θ should be chosen in dependence on the sign of $\Im\epsilon_{\mu s}$. We also stress that the analytical integration on the azimuth angle φ cannot be made in the general case because the value α_B depends on this variable.

This formula shows that there are two essentially different angular and spectral scales for characterization of the structure of the PXR reflex. One of them (low resolution scale – LRS) is defined by the angular dependence of the radiation coherent length:

$$(\delta\theta)^2 \leq |\chi_{\vec{h}}|, \quad (\delta\theta)_{\text{LRS}} \leq \sqrt{|\chi_{\vec{h}}|} \sim 10^{-2}-10^{-3}.\quad (28)$$

In the scope of LRS one can integrate Eq. (27) over one of the variable (θ or ω) and find the universal forms of distributions have been considered earlier in [14] and have been investigated in many experiments. Actually these distributions are not dependent on the dynamical effects and their amplitudes are defined by the value L_{abs} . An analogous picture takes place in the conventional low resolution diffraction when the intensity of the reflex is also proportional to L_{abs} [26].

But there is also a high resolution scale (HRS) in Eq. (27) which is defined by the Bragg condition for the emitted photons, that is,

$$|\alpha_B| \leq |\chi_{\vec{h}}|, \quad (\delta\theta)_{\text{HRS}} \simeq \frac{\delta\omega}{\omega_B} \leq |\chi_{\vec{h}}| \sim 10^{-5}-10^{-6}.\quad (29)$$

Certainly, the experimental investigation of such a thin structure of the PXR reflex should be connected with the two-crystal detector technique which is widely used in modern HRXRD but was firstly applied recently [25] for HRPXR analysis.

Therefore it is actual to consider the most essential features of the distribution (27). It proves that analogously to the kinematical PXR theory [14] and the conventional dynamical diffraction theory [26] this distribution can be represented in some universal form. Let us introduce new variables having the scale of the order of unity:

$$\begin{aligned}\eta_s &= \frac{-\beta\alpha_B + \chi_0(\beta - 1)}{\kappa_s}, \\ x_s &= \frac{\theta^2 + \theta_{ph}^2}{\kappa_s}, \\ \kappa_s &= 2C_s\sqrt{\beta\chi_{\bar{h}}\chi_{-\bar{h}}}.\end{aligned}\quad (30)$$

In these variables, the distribution of the PXR photons can be represented as

$$\frac{\partial^3 N_{hs}}{\partial \eta_s \partial x_s \partial \varphi} = \frac{e^2 v_s^2}{4\pi^2 \beta \sin \theta_B} I(\eta_s, x_s), \quad (31)$$

with little bit different scales but the same universal function $I(\eta, x)$ for both polarizations:

$$\begin{aligned}I &= \frac{x - u_{ph}}{x^2 |\eta + \text{sign}(\eta) \sqrt{\eta^2 - 1}|^2} \\ &\times \left| 1 - \frac{x}{x - \eta - \text{sign}(\eta) \sqrt{\eta^2 - 1} - u_0} \right|^2, \\ u_{ph} &= \frac{\theta_{ph}^2}{\kappa_s}, \quad u_0 = \frac{\chi_0}{\kappa_s}, \quad x > u_{ph}, \quad -\infty < \eta < \infty.\end{aligned}\quad (32)$$

Here the function $\text{sign}(\eta)$ is (+1) for $\eta > 0$ and (−1) for $\eta < 0$. Analogously to HRXRD the scans of the distribution on the dimensionless variables for HRPXR can be realized by various experimental scans both on angles and frequency.

Fig. 5 shows the characteristic form of the universal function $I(\eta, x)$. One can see that it includes the well known Darwin step [26] conditioned by the second factor in (32) and a more narrow Cherenkov peak due to the last term in (32). The ratio of amplitudes of these peaks depend on the values x , u_{ph} , u_0 .

It is easy to estimate by means of Eq. (32) the maximal dimensionless spectral intensity for PXR:

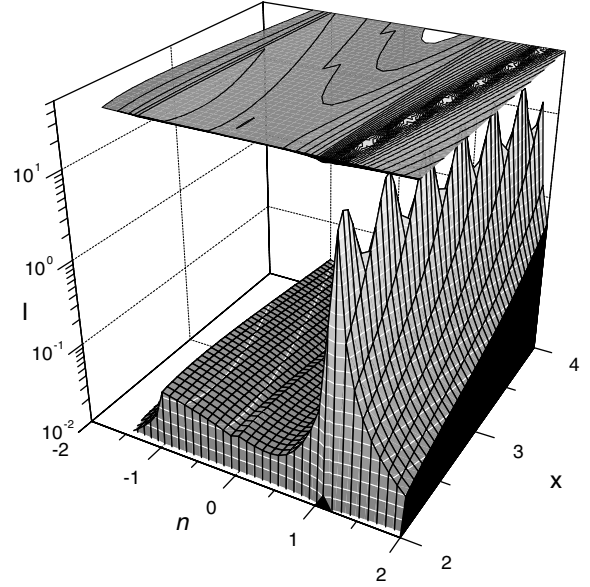


Fig. 5. Universal function for the HRPXR spectral-angular distribution represented as the three-dimensional image or in the form of a map (top of the picture) analogously to HRXRD [26]. The following parameters were used: $u_{ph} = 1.5$; $u_0 = 1.0 - i0.1$.

$$\begin{aligned}\left(\frac{\partial^3 N_{hs}}{\partial \eta_s \partial x_s \partial \varphi} \right)_{\max} &\simeq \frac{e^2 v_s^2}{4\pi^2 \beta \sin \theta_B} Q^2, \\ Q &= \frac{\Re \chi_0}{\Im(\chi_0 - \kappa_s)} \sim 10-100,\end{aligned}\quad (33)$$

which is achieved in the very narrow spectral range $\frac{\delta\omega}{\omega} \simeq \Im \chi_0 \sim 10^{-6}-10^{-7}$.

6. Conclusions

In this paper, we have investigated in detail the role of the dynamical effects for high resolution parametric X-radiation. The general formulae for description of this phenomenon and other radiation mechanisms in the same wavelength range are obtained. These expressions are also represented in a simplified analytical form which can make more clear the qualitative features of the effects considered and find the optimal conditions for their observation.

High spectral intensity of HRPXR could open new directions for application of such radiation

for crystal and nanostructure analysis. In particular, the estimation for the spectral intensity of the synchrotron radiation (SR) from one electron, analogous to (33), leads to the value $e^2/2\pi$ [6,35], which can be essentially less than for HRPXR. Certainly, in most cases the integral number of SR photons from the storage ring with a great electron current is much larger than the quantity of PXR quanta from linear accelerators with a quite small average current. But the applications of HRPXR as the X-ray source for structural analysis could be of interest for spectral-sensitive experiments where the spectral density of the radiation in the narrow spectral range is necessary. Some of the possible applications in this field are considered in [5–9].

Acknowledgements

The authors are grateful to the International Scientific Technical Center (Grant No. B-626) and Bruker AXS GmbH (Karlsruhe, Germany) for supporting this work.

References

- [1] V.G. Baryshevsky, I.D. Feranchuk, *J. Phys. (Paris)* 44 (1983) 913.
- [2] I.D. Feranchuk, *Kristallografiya* 24 (1979) 289.
- [3] V.G. Baryshevsky, *Nucl. Instr. and Meth. B* 122 (1997) 13.
- [4] V.G. Baryshevsky, I.D. Feranchuk, A.O. Grubich, A.V. Ivashin, *Nucl. Instr. and Meth. A* 249 (1986) 308.
- [5] I.D. Feranchuk, A.V. Ivashin, I.V. Polikarpov, *J. Phys. D: Appl. Phys.* 21 (1988) 831.
- [6] V.G. Baryshevsky, I.D. Feranchuk, *Nucl. Instr. and Meth.* 228 (1985) 490.
- [7] V.G. Baryshevsky, I.D. Feranchuk, *Phys. Lett. A* 76 (1980) 452.
- [8] V.G. Baryshevsky, I.D. Feranchuk, *Phys. Lett. A* 102 (1984) 141.
- [9] I.D. Feranchuk, A.V. Ivashin, *Kristallografiya* 34 (1989) 39.
- [10] V.G. Baryshevsky, *Channeling, Radiation and Reactions in Crystals under the High Energies*, Belarusian University, Minsk, 1982.
- [11] I.D. Feranchuk, *Doctor of Science Thesis*, Belarusian University, Minsk, 1985.
- [12] Yu.N. Adishchev, V.G. Baryshevsky, S.A. Vorob'ev, et al., *Pis'ma Zh. Eksp. Teor. Fiz.* 41 (1985) 295.
- [13] V.G. Baryshevsky, V.A. Danilov, I.D. Feranchuk, et al., *Phys. Lett. A* 110 (1985) 477.
- [14] I.D. Feranchuk, A.V. Ivashin, *J. Phys. (Paris)* 46 (1985) 1981.
- [15] K.-H. Brenzinger, C. Herberg, B. Limburg, et al., *Zh. Phys. A* 358 (1997) 107.
- [16] J. Freudenberger, H. Genz, V.V. Morokhovskiy, et al., *Phys. Rev. Lett.* 84 (2000) 270.
- [17] 5th Int. Symp. on Radiation from Relativistic Electrons in Periodic Structures, *Topical Issue of Nucl. Instr. and Meth. B* 201 (2003) 1.
- [18] H. Nitta, *Phys. Rev. B* 45 (1992) 7621.
- [19] H. Nitta, *Nucl. Instr. and Meth. B* 115 (1996) 401.
- [20] H. Nitta, *J. Phys. Soc. Jpn.* 69 (2000) 3462.
- [21] A. Caticha, *Phys. Rev. B* 45 (1992) 9641.
- [22] I.Ya. Dubovskaya, S.A. Stepanov, A.Ya. Silenko, A.P. Ulyanekov, *J. Phys.: Condens. Matter* 5 (1993) 7771.
- [23] N. Nasonov, V. Sergienko, N. Noskov, *Nucl. Instr. and Meth. B* 201 (2003) 67.
- [24] A.V. Schagin, *Radiat. Phys. Chem.* 61 (2001) 283.
- [25] H. Backe, C. Ay, N. Clawiter, et al., *Proc. Int. Symp. on Channeling – Bent Crystals – Radiation Processes*, Frankfurt am Main, 2003, p. 41.
- [26] U. Pietsch, V. Holy, T. Baumbach, *High-resolution X-ray Scattering*, Springer-Verlag, New York, 2004.
- [27] A.I. Akhezer, V.B. Berestetzky, *Quantum Electrodynamics*, Nauka, Moscow, 1969.
- [28] A.S. Davydov, *Theory of Solid State*, Nauka, Moscow, 1976.
- [29] I.D. Feranchuk, L.I. Gurskii, L.I. Komarov, et al., *Acta Cryst. A* 58 (2002) 370.
- [30] G.M. Garibyan, C. Yang, *Sov. Phys. JETP* 36 (1973) 631.
- [31] I.D. Feranchuk, B.A. Chevganov, *J. Phys. (Paris)* 43 (1982) 1687.
- [32] S.V. Blazhevich, G.L. Bochek, V.N. Gavrikov, et al., *Phys. Lett. A* 195 (1994) 210.
- [33] V.L. Kleiner, N.S. Nasonov, A.G. Safronov, *Phys. Stat. Sol. (B)* 181 (1994) 223.
- [34] V.V. Morokhovskiy, J. Freudenberger, H. Genz, et al., *Phys. Rev. B* 61 (2000) 3347.
- [35] I.D. Feranchuk, A.P. Ulyanekov, J. Harada, J.C.H. Spence, *Phys. Rev. E* 62 (2000) 4225.
- [36] J. Freudenberger et al., *Int. Workshop on Radiation Physics with Relativistic Electrons*, Tabarz, Germany, 1998, p. 198.
- [37] M.L. Ter-Mikaelian, *High Energy Electromagnetic Processes in Condensed Media*, Wiley, New York, 1972.